AFRL-ML-WP-TP-2006-449

DEVELOPMENT OF A DOVETAIL FRETTING FATIGUE FIXTURE FOR TURBINE ENGINE MATERIALS (PREPRINT)

Patrick J. Golden

MARCH 2006

Approved for public release; distribution is unlimited.

STINFO COPY

MATERIALS AND MANUFACTURING DIRECTORATE
AIR FORCE RESEARCH LABORATORY
AIR FORCE MATERIEL COMMAND
WRIGHT-PATTERSON AIR FORCE BASE, OH 45433-7750

REPORT DOCUMENTATION PAGE

Form Approved
OMB No. 0704-0188

1. REPORT DATE *(DD-MM-YY)*
March 2006

2. REPORT TYPE
Conference Paper Preprint

3. DATES COVERED *(From - To)*

4. TITLE AND SUBTITLE
DEVELOPMENT OF A DOVETAIL FRETTING FATIGUE FIXTURE FOR TURBINE ENGINE MATERIALS (PREPRINT)

5a. CONTRACT NUMBER
In-house

5b. GRANT NUMBER

5c. PROGRAM ELEMENT NUMBER
N/A

5d. PROJECT NUMBER
4347

5e. TASK NUMBER
RG

5f. WORK UNIT NUMBER
M02R3000

6. AUTHOR(S)
Patrick J. Golden

7. PERFORMING ORGANIZATION NAME(S) AND ADDRESS(ES)
Metals Branch, Behavior/Life Prediction Section (AFRL/MLLMN)
Metals, Ceramics, and Nondestructive Evaluation Division
Materials and Manufacturing Directorate
Air Force Research Laboratory, Air Force Materiel Command
Wright-Patterson Air Force Base, OH 45433-7750

8. PERFORMING ORGANIZATION REPORT NUMBER
AFRL-ML-WP-TP-2006-449

9. SPONSORING/MONITORING AGENCY NAME(S) AND ADDRESS(ES)
Materials and Manufacturing Directorate
Air Force Research Laboratory
Air Force Materiel Command
Wright-Patterson AFB, OH 45433-7750

10. SPONSORING/MONITORING AGENCY ACRONYM(S)
AFRL-ML-WP

11. SPONSORING/MONITORING AGENCY REPORT NUMBER(S)
AFRL-ML-WP-TP-2006-449

12. DISTRIBUTION/AVAILABILITY STATEMENT
Approved for public release; distribution is unlimited.

13. SUPPLEMENTARY NOTES
This is a work of the U.S. Government and is not subject to copyright protection in the United States.
This work has been submitted for publication in the proceedings of the 9th International Fatigue Congress (Fatigue 2006 Proceedings), Elsevier Ltd., publisher.
This paper contains color. PAO Case Number: AFRL/WS 06-0786, 22 Mar 2006.

14. ABSTRACT
A unique dovetail fretting fatigue fixture was designed and evaluated for testing turbine engine materials at room or elevated temperatures. Materials from the cold section and hot sections of military turbojet engines were chosen for testing. The new fixture was improved over the previously used dovetail fretting fatigue fixture by including direct measurement of contact forces, alignment control, and elevated temperature capability. Measurement of the shear component of the contact force was validated through an alternative instrumentation method. Initial tests reveal interesting variability in the behavior of the nickel based superalloy specimens.

15. SUBJECT TERMS
Fretting, Dovetail, Ti-6Al-4V, Nickel Based Superalloy, Elevated Temperature

16. SECURITY CLASSIFICATION OF: a. REPORT	b. ABSTRACT	c. THIS PAGE	17. LIMITATION OF ABSTRACT:	18. NUMBER OF PAGES	19a. NAME OF RESPONSIBLE PERSON (Monitor)
Unclassified	Unclassified	Unclassified	SAR	16	Patrick J. Golden
					19b. TELEPHONE NUMBER *(Include Area Code)* N/A

Standard Form 298 (Rev. 8-98)
Prescribed by ANSI Std. Z39-18

ORAL/POSTER REFERENCE: FT486

DEVELOPMENT OF A DOVETAIL FRETTING FATIGUE FIXTURE FOR TURBINE ENGINE MATERIALS

P. J. Golden

Materials and Manufacturing Directorate, Air Force Research Laboratory,
Wright-Patterson AFB, OH 45433, USA

ABSTRACT

A unique dovetail fretting fatigue fixture was designed and evaluated for testing turbine engine materials at room or elevated temperatures. Materials from the cold section and hot sections of military turbojet engines were chosen for testing. The new fixture was improved over the previously used dovetail fretting fatigue fixture by including direct measurement of contact forces, alignment control, and elevated temperature capability. Measurement of the shear component of the contact force was validated through an alternative instrumentation method. Initial tests reveal interesting variability in the behavior of the nickel based superalloy specimens.

KEYWORDS

Fretting, Dovetail, Ti-6Al-4V, Nickel Based Superalloy, Elevated Temperature

INTRODUCTION

Fatigue failures and high maintenance costs caused by fretting are a major concern in aircraft structures. Fretting occurs when two members are pressed together in contact and have a small oscillating relative displacement [1,2]. The wear and very high local stresses that occur near the edge of contact results in the nucleation of cracks and the reduction of the fatigue life of the material. It has been well documented that fretting occurs in lap joints of aircraft structures and at the dovetail blade and disk interface in turbofan engines. Additionally, fretting in dovetail joints is recognized as one of the costliest sources of in-service damage related to high cycle fatigue (HCF) in the US Air Force [3].

The objective of this work was to investigate fretting in a dovetail or fir tree type attachment that could be found in the fan, compressor, or turbine stages of a turbojet engine. A new testing apparatus has been developed to allow cyclic loading of a dovetail shaped specimen. This geometry results in the application of simultaneous cyclic normal and shear loading at the contact interface. Both room temperature and elevated temperature testing were conducted on Ti-6Al-4V and a Nickel based superalloy Rene’88DT, respectively. The fixture was designed to directly measure the contact forces on the specimen which is an improvement over previous dovetail fixtures [4,5]. In particular, the fretting pad holder design results in approximately 95% of the normal load transfer to a load cell while carrying all of the shear force. Also,

the replaceable fretting pads provide a significant cost advantage to replacement of entire dovetail fixtures after each test. Finally, an igniter based elevated temperature fixture is used for test temperatures of 650°C and higher. Testing and analysis was conducted on Ti-6Al-4V and Rene'88DT specimens and pads. Finite element method (FEM) analysis is used to confirm the measured contact loads and understand the behavior of the test.

EXPERIMENTAL PROCEDURES

Two sets of material have been used for this study. The first was a Ti-6Al-4V forged plate used in the US Air Force National High Cycle Fatigue Program. This material was tested at room temperature and is representative of materials found in the cooler sections of the turbofan engine such as the fan and early compressor stage blades and disks. The material was $\alpha+\beta$ forged then heat treated at 927°C for 1 hour, fan air cooled, and stress relieved at 704°C for 2 hours. The resulting microstructure was bimodal with a primary alpha grain size of approximately 20 μm (60% volume fraction) and the balance was lamellar $\alpha+\beta$. This microstructure can be seen in Moshier et al. [7]. This material was used for both the specimen and pad in the room temperature tests. The second set of materials was chosen for the elevated temperature testing and is representative of a turbine disk and blade pair. The specimen was machined from a forged disk made from a powder processed superalloy Rene'88DT. Details of this material can be found in Caton et al. [8]. The specimens were machined from material cut near the outer rim of the disk. The fretting pad paired with this specimen was machined from a single crystal alloy, Rene'N5, cast in an approximately 16 x 57 x 145 mm slab. Further details of this material can be found in [9,10]. The pads were machined from the slabs with the pressure face normal oriented along the growth (long) direction of the crystal. The 12.7 mm height direction of the pad was oriented in the thickness direction of the slab.

The specimen design was developed from previous work 5 and modified slightly with a longer grip section to fit the new fretting fatigue fixture and is shown in Figure 1. The fretting pad design is simply a scaled down version of that used by Murthy et al. 11. Both the specimen and the pad are 7.62 mm thick. The pad has a 5° taper which is matched by the slot in the pad holder discussed below. This taper allows the pad to become wedged into the slot and eliminate further slipping of the pad in the pad holder during the test. The contact profile chosen for this study was flat with rounded edges. The flat length is 3 mm and has 3 mm blending radii to an 11° taper. This type of rounded flat contact profile is representative of the interface between an engine blade and disk. Six Ti-6Al-4V specimens and twelve pads were machined for room temperature testing to compare to previous work on other fretting fatigue fixtures. Twenty-four Rene'88DT specimens and forty-eight Rene'N5 pads were machined for elevated temperature testing. An additional four IN718 specimens and eight pads were machined for development of the elevated temperature setup. To date only three of the Ti-6Al-4V specimens and five of the Rene'88DT specimens have been tested. Testing was constant amplitude loading with a remote load ratio of 0.1. All tests were performed at 20 Hz to match the previous room temperature Ti-6Al-4V testing, and to develop an initial load-life curve for Rene'88DT. Future tests with Rene'88DT are planned at both 20 Hz and 0.33 Hz (20 cpm) to study frequency effects.

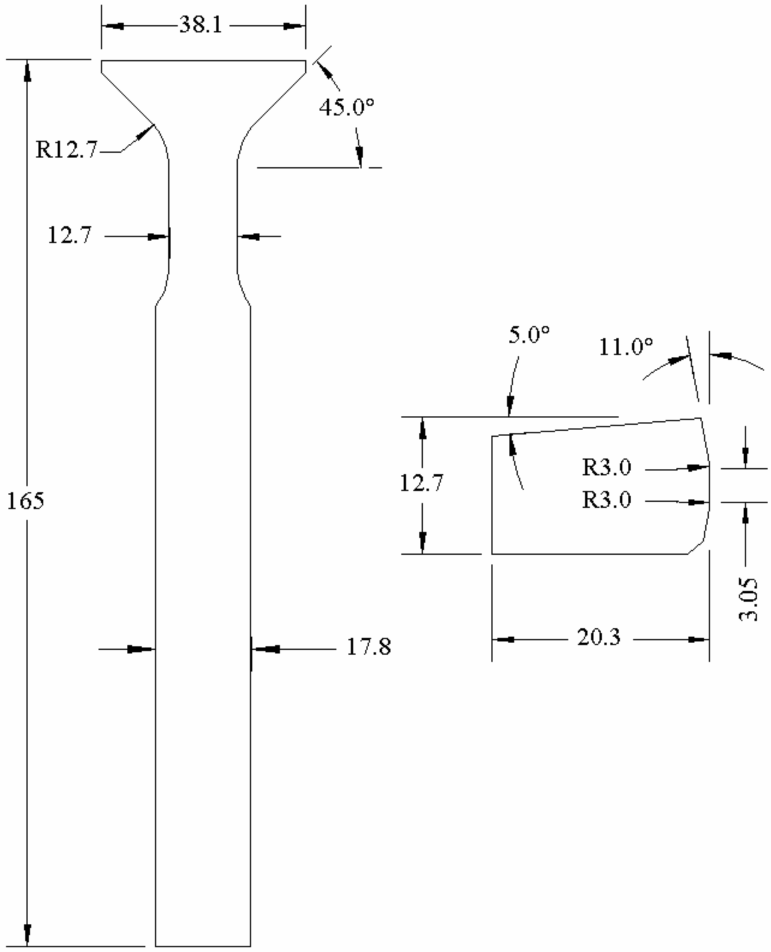

Figure 1: Drawing and dimensions (mm) of fretting specimen and pad

The motivation for a new fretting fatigue fixture for testing dovetail type specimens was two fold. First, improved methods of instrumentation and alignment were needed. The previous dovetail fretting fatigue fixture was machined from a block of steel leaving no flexibility for alignment of the pad-specimen interface or for direct measurement of the contact loads. Second, an elevated temperature capability was needed for the application of interest. Heating an elevated temperature version of the previous dovetail fretting fatigue fixture was considered, however, instrumentation would have been too difficult. A new dovetail fretting fatigue fixture was designed and machined as shown in the Figure 2 drawing. This design is composed of several parts. The top piece is a 50.8 x 63.5 x 381 mm steel beam that serves as the base for the other components of the fixture and attaches to the load cell and top of the servo-hydraulic test frame by a threaded rod. The outer truss structure is made of 25.4 x 38.1 mm cross-section steel members linked by ½ inch shoulder bolts. The inner structure has two IN718 pad holders which are each bolted to the base structure by four 3/8-24 bolts. The pad holders have a slot machined to accept the fretting pads shown in Figure 2 and described above. The central part of the pad holders are composed of two 2.5 mm thick webs. The webs are designed so that the pad holders are stiff in the transverse or shear loading direction, but very compliant in the normal loading direction. Behind each pad holder is a miniature 45 kN load cell that supports the normal component of the contact load. In order to remove any "play" in the system, a small plate and a ¾" set screw is located behind each load cell. These set screws are used to preload the system by pushing the load cells into the pad holders. This forces the load cells into contact with the pad holders and puts tension on the pin joints of the truss. Next, four plates are mounted to the base on each side of the pad holders for alignment (not shown in the drawing). Before fully tightening the bolts that attach the pad holders to the base, alignment screws are used to adjust the position of the pad holders. Pressure sensitive film is used to check the quality of the contact between the specimen and pads, and the alignment is adjusted as needed. Finally, heating of the specimen and pads is achieved through the use of furnace igniters mounted on either side and surrounded by ceramic blocks and

insulation. Temperature is controlled using thermocouples and a Barber-Colman controller to modulate the voltage to the igniters.

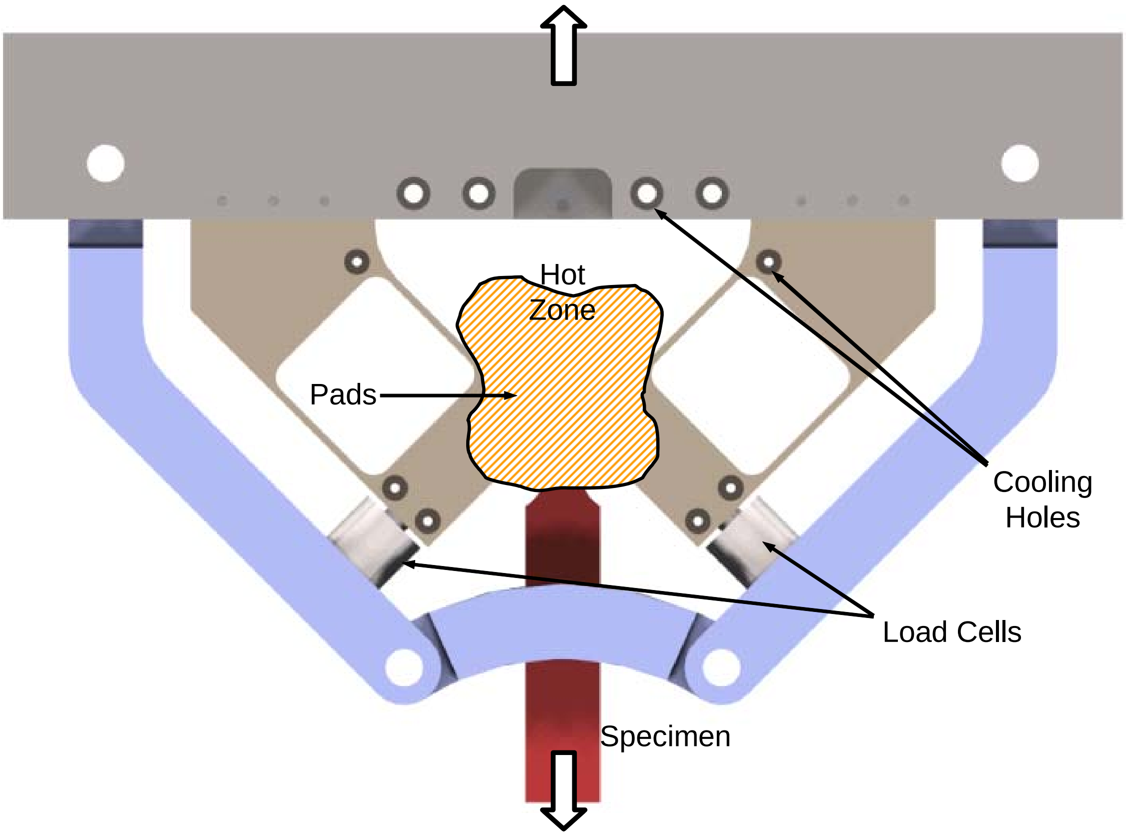

Figure 2: Drawing of the elevated temperature dovetail fretting fatigue fixture

As described above, miniature load cells are used to carry the normal force from the contact interface to the outer structure of the fretting rig. 100% of the normal force cannot transfer through to the load cells, since a portion of the normal force is carried by bending of the pad holder webs. A finite element model of the pad holders was created to estimate the load transfer ratio to the load cells. Figure 3 is a mesh very similar to that used to calculate this static problem, however, this particular mesh was used to develop a non-linear contact mechanics solution and it includes the fretting specimen. Rather than model the entire system several boundary conditions were used to be representative of the actual system. First, symmetry was imposed. Second, rather than model the attachment of the pad holder to the base it was assumed to be near rigid and a fixed boundary condition was imposed at the top edge of the pad holder. Finally, rather than model the load cell and outer truss a spring was used that accounted for the stiffness of the truss and the spring. The stiffness of this spring was determined to be $7.50\text{x}10^7$ N/m. The load cell stiffness was measured experimentally on a hydraulic load frame and the stiffness of the truss (under pre-load) was calculated to be greater than 10 times that of the load cell. A normal force in conjunction with a shear force was applied to the fretting pad and the force in the spring was determined to equal approximately 95% of the applied normal force. Therefore, for all instrumentation calculations a load transfer ratio of 95% was assumed.

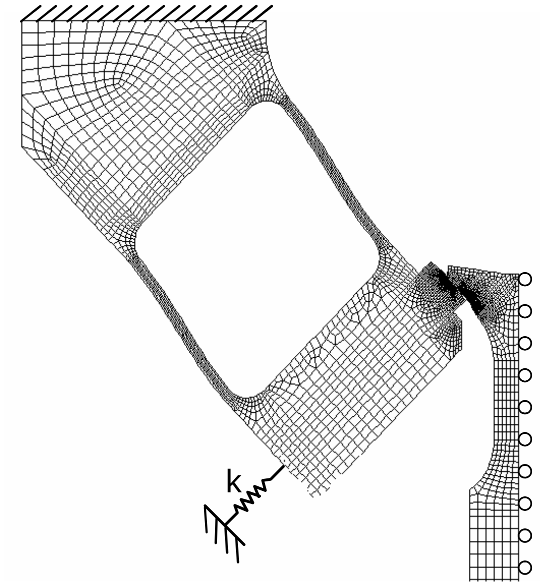

Figure 3: Finite element mesh used for contact modeling and for design of the pad holder (displacement scaling of 30x)

The load transfer calculation defines the relationship between the normal force, P, and the measured load in the miniature load cell, F_{mlc}. This relationship is defined by Equation 1 where LT is the fraction of normal load transferred to the load cell (0.95). Additionally, the shear force, Q, between the specimen and the pad can be calculated from the applied remote load, F_y, and P (or F_{mlc}) with Equation 2. Symmetry must be assumed in this calculation so that the remote vertical force is equally divided between the left and right contacts. In general, the miniature load cell measurements have less than 5% difference. In practice the average value from the two miniature load cells was used in Equation 1. The calculation of Q was checked experimentally on several of the room temperature tests. The thing webs on one of the fretting pad holders were instrumented with strain gages on the front and back of both webs. The gages were placed at equal positions along the length of the webs and configured in four separate quarter bridges which allowed the average axial strain in each web to be calculated. The results were then used to calculate the axial force transferred through the pad holder webs as shown in Equation 3. Here, E is Young's Modulus, A is the total cross-sectional area of both webs, and ε_i are the strains. A simple free body diagram shows that the sum of the axial forces in the webs is equal to the shear contact force, Q.

$$P = \frac{F_{mlc}}{LT} \tag{1}$$

$$Q = \frac{F_y}{2\cos 45^\circ} - P \tag{2}$$

$$Q = EA\frac{(\varepsilon_1 + \varepsilon_2 + \varepsilon_3 + \varepsilon_4)}{4} \tag{3}$$

The mesh shown in Figure 3 was used to perform a contact mechanics analysis on the pad and specimen interface. To date only the Ti-6Al-4V on Ti-6Al-4V material pair has been modeled. The contact element mesh size was 50 μm resulting in approximately 65 elements in contact. The average coefficient of friction, μ, was an additional input to this analysis. It was varied from 0.3 to 0.75 and was determined empirically from test data. A typical value of μ for Ti-6Al-4V from this test setup was 0.7. Three load steps were used in the analysis (max, min, and max). The loads were applied remotely as a pressure on the bottom edge of the specimen. The output of this analysis was the pressure and shear tractions along the contact. These tractions were then integrated to determine the normal, P; shear, Q; and moment, M at each load step and substep in the analysis. Although 65 elements in contact was not enough mesh

refinement to accurately determine local stresses, it has been deemed to be sufficient to determine contact forces through integration of the tractions [12].

RESULTS AND DISCUSSION

The results of the room temperature Ti-6Al-4V and elevated temperature Rene'88DT dovetail fretting fatigue tests are reported in Figure 4. The lives of the three Ti-6Al-4V specimens ranged between 40,000 and 300,000 cycles which will allow comparison with previous testing at similar lives. The five Rene'88DT specimen results included two run-outs at lower loads, two repeats at a maximum load of 24 kN, and a failure at a maximum load of 28 kN. Although only two repeats were performed at 24 kN, the results showed a wide scatter with failure ranging between 118,400 and 1.38 million cycles. One of the objectives of future testing will be to measure the variability in the life at a single loading condition and to study the influences on that variability. Ten to fifteen repeated tests will be performed at the same maximum load, load ratio, temperature, and frequency. Variables that will be studied are the measured contact loads, the average coefficient of friction, the evolution of the loads and coefficient of friction over the course of the test, and the resulting damage and crack formation. Some initial study of variability between the tests performed at 24 kN will be discussed below.

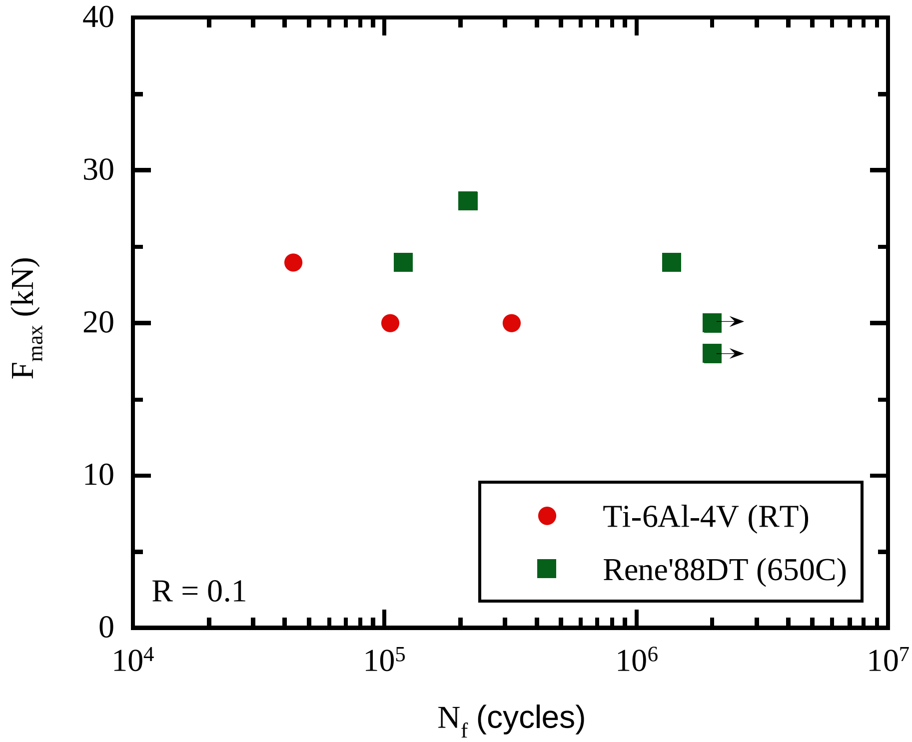

Figure 4: Test results from dovetail fretting fatigue fixture

Figure 5 is a comparison between the two measurements of the contact shear force Q calculated by Equations 1-3. The first method is based solely on the load cell measurements. This method is much more practical, particularly at elevated temperature when instrumenting the pad holder webs with high temperature strain gages and thermocouples would be difficult and unreliable. The intent of the second method, strain gage instrumentation of the pad holder webs, was solely to validate the miniature load cell calculation. This is ultimately a validation of the load transfer quantity, LT, which was calculated with FEM. The dashed line represents perfect agreement. It can be seen that the two methods match very closely. The maximum difference at maximum load is less than 5% and the difference in slope is less than 5%. These differences could be the result of error in the strain gage locations, lack of symmetry in the test setup, or incorrect value of the load transfer ratio, LT. The slope of this line can be adjusted by changing the assumed value of LT from the calculated value of 0.95. To reach perfect agreement, however, LT

must equal 1.08. That is clearly not a possible solution so the calculated value of 0.95 was used for all subsequent tests.

Figure 6 is a plot of the shear force Q versus the normal force P for a Ti-6Al-4V test. The solid line trace represents a few cycles of data recorded early in the experiment after the coefficient of friction had stabilized. The open squares are numerical results from the ABAQUS FEM model of the contact. The dashed lines represent the bounds of possible Q and P combinations defined by $|Q| \leq \mu P$, where μ is the average coefficient of friction. The plots of Q versus P are very good for showing the two modes of fretting, gross slip and partial slip. Gross slip occurs when all parts of the contact interface are slipping and by definition $|Q| = \mu P$. The initial ramp up in load occurs under gross slip as shown by the FEM results. The dovetail specimen gets wedged between the pads in the same manner as a turbine blade slides out in the dovetail slot. Once the load reverses the dovetail remains wedged in place and the contact is now in partial slip. The slope of Q vs. P during partial slip is dependent on the applied loading configuration (uniaxial or biaxial) and the compliance of the specimen and fixtures. Figure 6 shows that the FEM model matches the experimental value of this slope very well. In this test, the contact remains in partial slip throughout the remainder of the test. If unloading were to continue further or if the coefficient of friction were to decrease, the contact would return to gross slip.

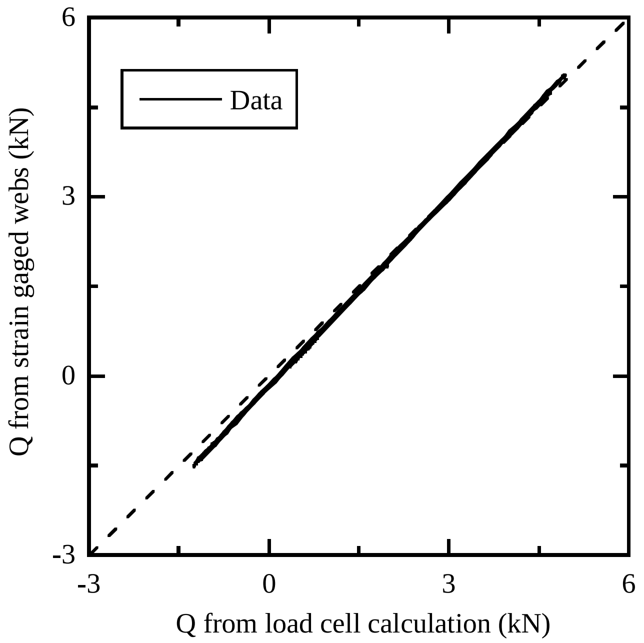

Figure 5: Comparison of shear load calculated by two methods. The load cell calculation depends on an FEM load transfer coefficient.

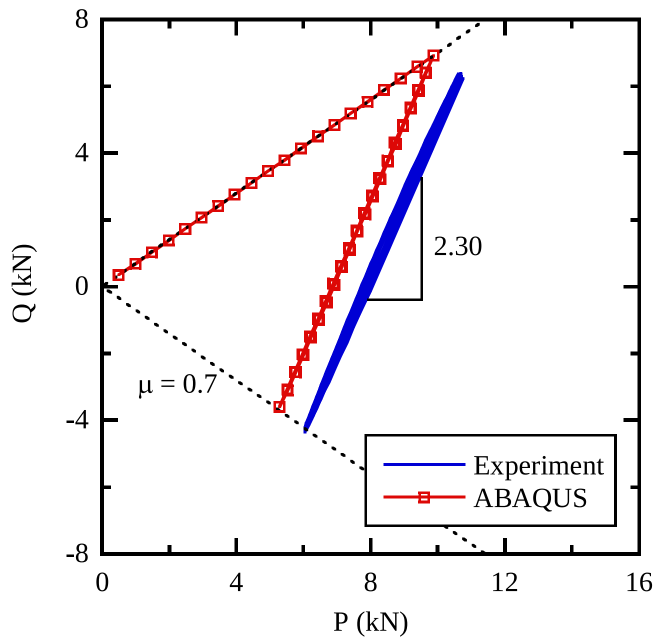

Figure 6: Ti-6Al-4V FEM results compared to test results. Note the very close match between the test and model Q versus P slopes during partial slip.

Figure 7 is an example of Q versus P for a Rene'88DT specimen, identified as 05-952, with a maximum load of 24 kN and R = 0.1. The test lasted 118,400 cycles and was in partial slip throughout the test. The maximum value of Q/P during the test was about 0.75 which bounds the average coefficient of friction, $\mu \geq 0.75$. The second set of data on this plot, which was measured at 118,000 cycles, clearly shows a change in slope and a curvature in the load path. This resulted from a change in compliance of the specimen due to a crack growing from the edge of contact on one side of the specimen. This effect was measurable during the test and was used to detect cracks. A second Rene'88DT specimen (05-953) was also tested with a maximum load of 24 kN and R = 0.1. The measured contact loads from this specimen are plotted in Figure 8. Initially (1000 cycles), the load trace was very similar to specimen 05-952 but with a slightly different Q versus P slope during partial slip. As the test progressed, however, the load trace began to change. After 1 million cycles the load trace had moved to higher values of Q and lower P and the load trace was an open loop rather than a straight line. By the end of the test, at 2 million cycles, the load trace indicated a classic gross slip hysteresis. The average coefficient of friction had dropped from 0.75 to 0.5 and gross slip was occurring on each cycle.

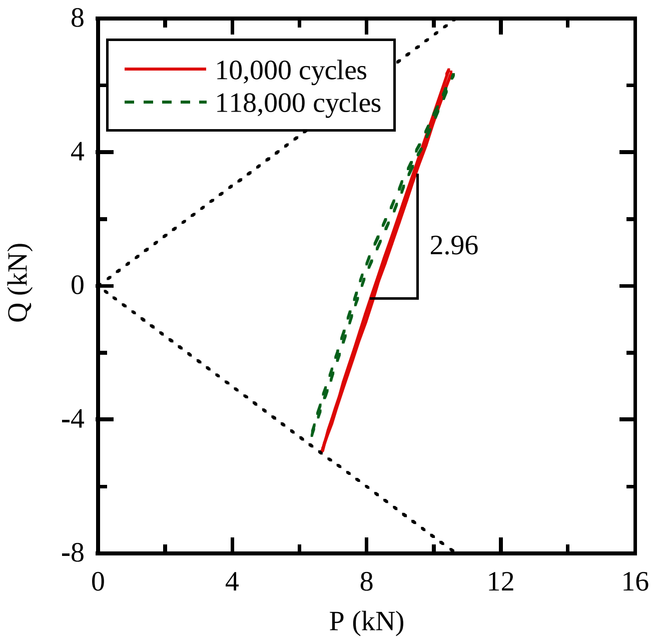

Figure 7: Q/P load history for test (05-952) that formed a large crack and failed near 118,000 cycles

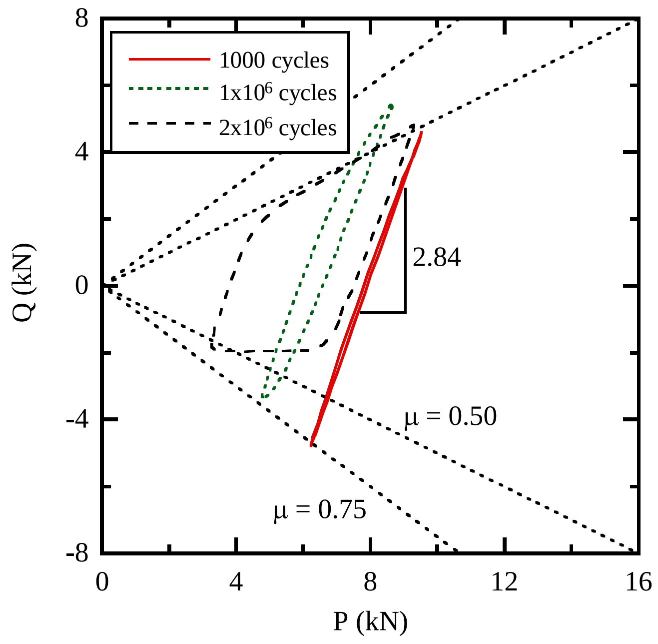

Figure 8: Q/P load history for specimen (05-953) with same applied loading as Figure 4. It did not fail and the surface interaction switched to gross slip near 1 million cycles.

Figures 9 and 10 are photographs of the fretting scars from the two specimens 05-952 and 05-953 discussed above. Specimen 05-952, which failed early, has a racetrack pattern type of scar. Dark bands around the edges of contact indicate wear in the slip zones which surround the contact patch during partial slip conditions. Specimen 05-953, however, was a 2 million cycle run-out that did not form a crack that grew to failure. The wear scar, like the load traces, indicated severe damage through the contact patch due to gross slip or fretting wear. It was unclear why these two specimens machined from identical materials and tested at identical temperatures, contact loads, and frequencies behaved so differently. It seemed that if the test did not form a crack early in life the surface interaction changed. This was likely due lubrication of the interface with the build up of fretting debris. Planned analysis of the stress, fatigue, and crack growth of these specimens will help increase understanding of the variability of the life.

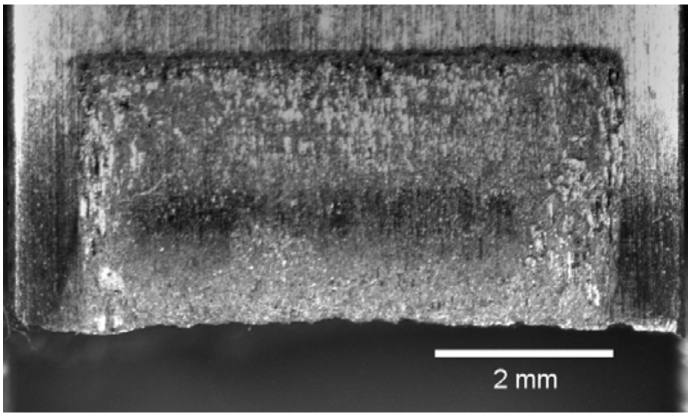

Figure 9: Fretting scar for specimen 05-952 showing typical partial slip fretting scar

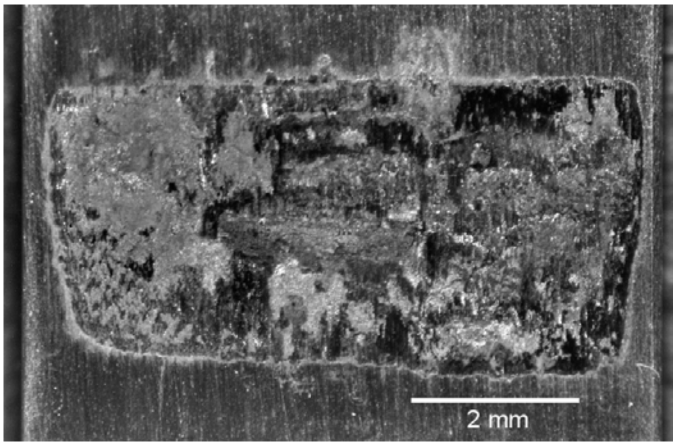

Figure 10: Fretting scar from specimen 05-953 showing wear damage due to gross slip after 2 million cycles

CONCLUSIONS

A unique dovetail fretting fatigue experimental setup was developed to study fretting of turbine engine materials. The design of this experimental work built on the capabilities of previously developed systems.

Important capabilities added to this system include heating elements capable of simulating conditions in the attachment region of the turbine. Also, direct force measurements for improved determination of the contact forces are obtained through miniature load cells mounted in the fixture. Finally, fine tuning of the alignment between the specimen and pads is possible with set screw adjustment of the pad holder orientation. Several conclusions can be made from the initial tests that have been conducted with this new system. First, the specimens fail at the expected location and the fretting scars appear as expected. The elevated temperature system works and satisfactorily controls the temperature of the specimens near the contact interface. The initial set of Rene'88DT tests had interesting results including large variability in life and surface condition at a single test condition. Further testing is planned to study the causes of this variability.

ACKNOWLEDGEMENTS

This work is supported by the DARPA Engine System Prognosis program with Dr. Leo Christodoulou as program manager. The author would like to acknowledge Professor Farris and students from the School of Aeronautics and Astronautics at Purdue University for their assistance with the design of this fretting fatigue fixture. The author would also like to acknowledge General Electric Aircraft Engines for supplying the Rene'88DT and Rene'N5 materials used in this study.

REFERENCES

1. Johnson, K.L. (1985) *Contact Mechanics*. Cambridge University Press, Cambridge.
2. Hills, D.A., Nowell, D. (1994) *Mechanics of Fretting Fatigue*. Kluwer Academic Publishers, Dordrecht, the Netherlands.
3. Nicholas, T. (1999) *Int J Fatigue*, 21(S), S221-31.
4. Conner, B.P., Nicholas, T. *ASME J. Eng. Mat. Tech*, in press.
5. Golden, P.J., Nicholas, T. (2005) *Fatigue Fract. Eng. M*. 28, 1169-75.
6. Murthy, H., Rajeev, P.T., Okane, M., Farris, T.N. In: *Fretting Fatigue: Advances in Basic Understanding and Applications, STP 1425*, Y. Mutoh, S.E. Kinyon, and D.H. Hoeppner, (Eds)., American Society for Testing and Materials International, West Conshohoken, PA, 2002.
7. Moshier, M.A., Nicholas, T., Hillberry, B. (2001) *Int. J. Fatigue*, 23, S253-58.
8. Caton, M.J., Jha, S.K., Rosenberger, A.H., Larsen, J.M. (2004) In: *Superalloys 2004*. K.A. Green, T.M. Pollock, H. Harada, T.E. Howson, R.C. Reed, J.J. Schirra, and S. Wanston, (Eds). The Minerals, Metals and Materials Society (TMS).
9. Nazmy, M., Kunzler, A., Denk, J., Baumann, R. (2002) *Scripta Mater.*, 47, 521-525.
10. Walston, W.S., OHara, K.S., Ross, E.W., Pollock, T.M., Murphy, W.H. (1996) In: *Superalloys 1996*. R.D. Kissinger, D.J. Deye, D.L. Anton, A.D. Cetel, M.V. Nathal, T.M. Pollock, D.A.Woodford, (Eds). The Minerals, Metals and Materials Society (TMS).
11. Murthy, H., Rajeev, P., Okane, M., Farris, T.N. (2002) In: *Fretting Fatigue: Advances in Basic Understanding and Applications, STP 1425*, Y. Mutoh, S.E. Kinyon, D.H. Hoeppner, (Eds). American Society for Testing and Materials International, West Conshohocken, PA, 41-48.
12. Golden, P.J., Calcaterra, J.R. *Tribology International*, in press.